MALAYSIAN JOURNAL OF SCIENCE
MJS
ISSN 1394 - 3065

2nd Euro-Asia Conference on CO_2 Capture and Utilization (EACCO2CU2022) Special issue

Malaysian Journal of Science 43 (Special Issue 1): 15-19 (July 2024) https://mjs.um.edu.my

EXPERIMENTAL INVESTIGATION OF AMINE-BASED GRAPHENE NANOSUSPENSION FOR CO_2 ABSORPTION

Nur Azni Farhana Mazri[1a], A Arifutzzaman[2b*], Mohamed Kheireddine Aroua[3a,c]

Abstract: Absorption is the most widely used carbon dioxide (CO_2) removal technology. The CO_2 absorption performance of monoethanolamine (MEA), the most commonly used CO_2 absorbent, can be improved by suspending nanoparticles. This work examined the performance of graphene nanoplatelets (GNPs) as additives to enhance CO_2 absorption in MEA. The GNPs were characterized by HRTEM, FTIR, and XRD. The study examined the influence of GNP concentrations on CO_2 absorption at room temperature. The images from HRTEM confirmed that the implemented graphene consists of several layers of graphene sheets. Increasing the loading of particles increased the solubility of CO_2 until the optimum concentration was reached. From this work, it is evident that incorporating GNPs into MEA enhances the CO_2 absorption performance of MEA. Thus, the addition of nanoparticles to the absorbent can enhance its CO_2 absorptivity.

Keywords: 2D Nanomaterials, Graphene, Nanosuspensions, Amine, CO_2 absorption.

1. Introduction

Absorption is one of the methods used for acid gas removal. Carbon dioxide (CO_2), one of the acidic gases, is derived from natural sources and anthropogenic emissions. CO_2 absorption is one of the techniques used for post-combustion CO_2 capture. Ochedi et al. (Ochedi, Yu, Yu, Liu, & Hussain, 2021) mentioned that the capability, experience, and reliability of the technique make it the most promising CO_2 capture technology. Monoethanolamine (MEA), a primary amine, has been extensively used and studied as a CO_2 absorbent. One mole of CO_2 will react with two moles of amines to form carbamate, as shown by the following equation:

$$CO_2 + 2RNH_2 \leftrightarrow RNHCOO^- + RNH_3^+ \quad (1)$$

The disadvantages of MEA include corrosivity, high toxicity, regeneration energy requirements, vapor pressure and volatility, low CO_2 capacity, and the need for additional operational equipment, which undermine the effectiveness of MEA (Hamidi, Farsi, & Eslamloueyan, 2018; Ramezani, Mazinani, & Di Felice, 2021; Seo, Lages, & Kim, 2020). An ideal absorption solvent should have high CO_2 capacity, chemical and thermal stability, fast reaction rates, and low absorption heat, regeneration energy, toxicity, and volatility (Hamidi et al., 2018; Ramezani et al., 2021). In this regard, nanofluid is one of the approaches identified to overcome the problem. Suspension of nanoparticles in a base fluid produces nanofluid.

Several studies have shown that adding nanoparticles can enhance CO_2 capture. Seo et al. (Seo et al., 2020) employed a nickel nanoparticles-MEA system for CO_2 absorption in two microfluidic platforms: a microreactor and a long serpentine channel. They reported an increase of 34% and 54% in the rate of CO_2 absorption in the microreactor and long serpentine channel, respectively. $TiO(OH)_2$ has also been reported to accelerate the CO_2 absorption of MEA (Lai et al., 2018). Mohammadpour et al. (Mohammadpour, Mirzaei, & Azimi, 2019) employed a dimensionless number system to quantify the effect of additives on the CO_2 absorption of MEA. Among the carbon additives used in the study, graphene oxide (GO) showed the most significant impact on enhancing solubility and mass transfer rate. Source (Rahimi, Riahi, & Abbasi, 2020) suspended pristine and modified carbon nanotubes (CNTs) in different base fluids, where all types of CNT addition increased CO_2 absorption. In the GO-SDS-MEA system (mohammadpoor, Mirzaei, Azimi, & ghomshe, 2018), the addition of GO increased the mass transfer coefficient and CO_2 molecular diffusion, with a linear relationship with temperature and an inverse relationship with pressure.

In this work, we evaluated the performance of graphene nanoplatelets (GNPs) as additives to enhance CO_2 absorption in MEA. The influence of the volume fraction of GNPs at room temperature was investigated. To eliminate the influence of dispersants, the GNP-MEA nanofluids were prepared using the ultrasonic dispersion method without adding any dispersant.

Authors information:
[a]*Centre for Carbon Dioxide Capture and Utilization (CCDCU), School of Science and Technology, Sunway University, No. 5, Jalan Universiti, Bandar Sunway, 47500 Petaling Jaya, Selangor, Malaysia. Email:* kheireddinea@sunway.edu.my[3]
[b]*Tyndall National Institute, University College Cork, Lee Maltings, Cork, T12 R5CP, Ireland. Email:* arifutzzaman.rahat@tyndall.ie[2]
[c]*School of Engineering, Lancaster University, Lancaster LA1 4YW, United Kingdom. Email:* kheireddinea@sunway.edu.my[3]

*Corresponding author: arifutzzaman.rahat@tyndall.ie[2], kheireddinea@sunway.edu.my[3]

Received: February 7, 2024
Accepted: May 7, 2024
Published: July 31, 2024

DOI: https://doi.org/10.22452/mjs.vol43sp1.3
Malaysian Journal of Science 43 (Special Issue 1): 15-19 (July 2024)

2. Methodology

2.1. Materials

This study used GNPs (Sigma-Aldrich), MEA (Merck), CO_2 (Alpha Gas Solution, Malaysia), and deionized water (DW).

2.2. Synthesis of Nanofluids

The nanofluids used in this study were prepared using the two-step method, where the nanoparticles were introduced into the base fluid. The stock solution of the base fluid was prepared by stirring a mixture of MEA and DW for 30 min. The GNPs needed were then measured so that the resultant nanofluids would have the following volume fractions (ϕ): 0.01, 0.03, and 0.05. Before the nanofluids were sonicated for 1 h via an ultrasonic bath, where the sonication process was conducted for 15 min for each session, the GNP-MEA dispersions were stirred for 30 min. The temperature of the sonication process was kept constant at 25 ± 2 °C throughout the process. No dispersing agent was used in the preparation to prevent any interference with CO_2 absorption.

3. Characterization

3.1 High-Resolution Transmission Electron Microscope

A FEI-Tecnai G^2 20 S-Twin high-resolution transmission electron microscope (HRTEM) was employed to analyze the morphologies and geometric specifications of the GNPs. The preparation of the sample involves 20-min sonication of 1 mg of GNP suspension in isopropyl alcohol, followed by overnight air-drying on a copper grid (Formvar-carbon coated, 300 mesh).

3.2 Fourier Transform Infrared Spectroscopy

An attenuated total reflectance (ATR)-equipped VERTEX 70v Fourier transform infrared (FTIR) spectrometer (Bruker) was employed to identify the functional groups of the GNPs. The spectra of the samples were acquired in the range of 4000–400 cm^{-1} and with a resolution of 4 cm^{-1}.

3.3. X-ray Diffraction

A Miniflex X-ray diffractometer (Rigaku) equipped with Kβ-filtered Cu-Kα radiation (λ = 0.1544 nm) generated at 15 mA and 40 kV was used for X-ray diffraction (XRD) analysis. The diffractogram was recorded in the 2θ range between 10° and 90° with a scanning speed of 6° min^{-1}.

3.4. CO_2 Absorption

Fig. 1 shows the setup used for the CO_2 absorption experiments, which is identical to the one used by (Abdul Samat, Yusoff, Aroua, Ramalingam, & Kassim, 2019). CO_2 flowed from (I) to (II), where it was heated and pressurized to the required conditions. Then, 20 mL of the sample was added into (IV) and heated to the required temperature. The temperature of (II) and (IV) was kept constant during the experiment. The pressure of CO_2 was simultaneously recorded by (VII) during the experiment until

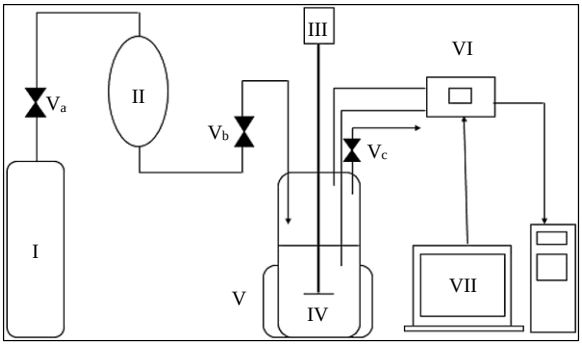

Figure 1. A diagram of the experimental setup: (I) gas cylinder, (II) gas reservoir, (III) motor, (IV) high-pressure reactor cell, (V) water bath, (VI) controller, (VII) computer, (V_a) control valve, (V_b) needle valve, and (V_c) pressure relief valve.

the equilibrium was reached, where the pressure remained constant for at least 30 min. The CO_2 absorptivity of the prepared nanofluids was determined using the CO_2 pressure drop (Eqn. (3)), expressed as CO_2 solubility (mol of CO_2 /mol of solvent).

$$PV = nRT \quad (2)$$

Table 1 Experimental conditions of CO_2 absorption

Parameters	Value
Mass concentration of MEA solution	30%
Pressure of CO_2	50, 125, and 200 psi
Temperature of thermostatic water bath	26 °C
Ultrasonication time	1 h
Volume of nanofluids	20 mL
Volume fraction of GNPs	0.01, 0.03, and 0.05

$$\Delta n = \frac{P_1 V_1}{RT} - \frac{P_2 V_2}{RT} \quad (3)$$

Where P1 and P2 are the initial and final pressures (Pa), respectively, V1 is the volume of the gas reservoir (m^3), V2 is the volume of the system except the reactor cell (m^3), R is the gas constant ($m^3 \cdot Pa \cdot K^{-1} \cdot mol^{-1}$), and T is the temperature (K). The experimental conditions of CO2 absorption are summarized in Table 1.

4. Results and Discussion

4.1. Characterization

4.1.1. HRTEM Analysis

Fig. 2 shows the optical microscopy images of GNPs. The flat multi-layered graphene sheets are rough and jagged (Fig. 2(a)). Also, the edges of the sheets appear smooth but irregular in some areas (Fig. 2(a)). The interlayer distance of the graphene sheets

DOI: https://doi.org/10.22452/mjs.vol43sp1.3
Malaysian Journal of Science 43 (Special Issue 1): 15-19 (July 2024)

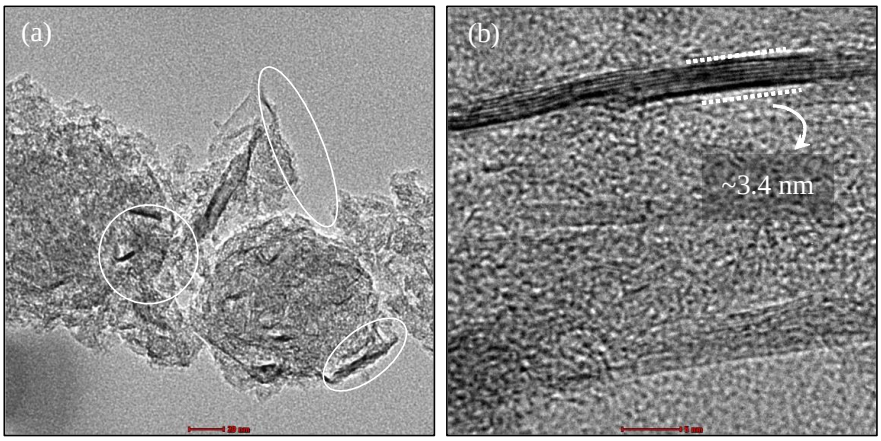

Figure 2. TEM images of GNPs

was found to be approximately 340 pm (Fig. 2(b)), in agreement with the XRD results (Fig. (3)).

4.1.2. XRD Analysis

Fig. 3 shows the XRD patterns of GNPs. It can be seen that a strong peak was emitted at 2θ = ~26.3°, which is related to the [002] plane (Gomari, Esfandeh, & Ghasemi, 2017). The wide peak at 2θ = ~43.0° and the small peak at 2θ = ~54.2° of the XRD patterns could be ascribed to the [100] and [004] peaks, respectively (Kumar et al., 2018). The interlayer distance $d_{(002)}$ is 0.34 nm, as calculated by Bragg's law (Eqn. (4)). The value is in agreement with the $d_{(002)}$ value of graphite (Farinre et al., 2022).

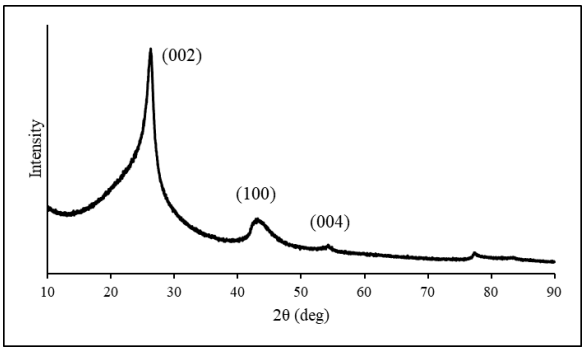

Figure 3. XRD crystallographic patterns of GNPs.

$$d_{hkl} = \frac{\lambda}{2sin\theta} \quad (4)$$

4.1.3. FTIR Analysis

Fig. 4 illustrates the bonds and their respective wavelengths of GNPs. The C=C peak was observed at 1564 cm^{-1}. As seen in the spectra, a negligible amount of oxygen groups can be found in the GNPs.

4.1.4 Stability Analysis

Nanofluid stability is important for CO_2 absorption as it influences the mass transfer enhancement mechanisms. The MEA-GNP nanofluids used in this work were prepared via the two-step method, where the production and dispersion of the nanoparticles occur in two separate steps. To achieve a uniform colloidal dispersion, ultrasonication was also employed to prepare the nanofluids. Fig. 5 visualizes the stability performance of the prepared MEA-GNP nanofluids, where the GNPs were found to be sedimented 72 h after the preparation (Fig. 5(b)).

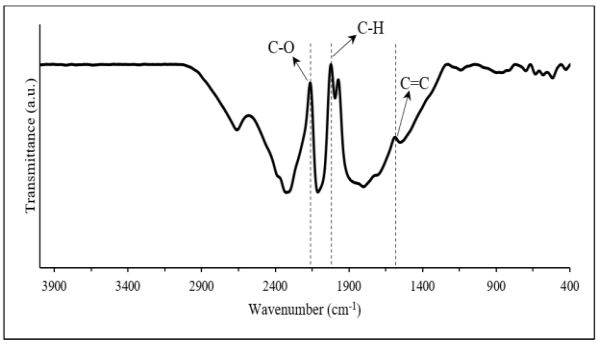

Figure 4. FTIR spectra of GNPs.

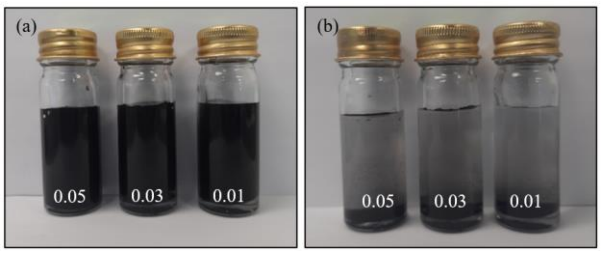

Figure 5. The stability of MEA-GNP nanofluids (a) after preparation and (b) after 72 h.

4.2. CO_2 Absorption Study

The absorption of CO_2 in the pure MEA solution is about 0.62 mol/mol MEA, which agrees with the solubility of CO_2 in MEA (0.64 mol/mol MEA) as reported by Jiang et al. (Jiang, Zhao, Zhuo, & Wang, 2014). Fig. 6 indicates that the CO_2 solubility of GNP-MEA nanofluids was slightly higher than the base fluid, MEA. The GNP addition improved the CO_2 solubility of MEA by 2%. The effect of GNP loading on the CO_2 solubility of MEA was then investigated. The CO_2 solubility of GNP-MEA nanofluids increased until reaching

DOI: https://doi.org/10.22452/mjs.vol43sp1.3
Malaysian Journal of Science 43 (Special Issue 1): 15-19 (July 2024)

the optimum level of ϕ = 0.03 and then decreased. The increase in CO_2 solubility of MEA can be explained by the generally acknowledged mass transfer enhancement mechanisms, the hydrodynamic effect, the shuttle effect, and the inhibition of bubble coalescence (Zhang et al., 2022). The shuttle effect can be explained as the nanoparticles acting as a shuttle for the adsorbed gas, transferring the gas repetitively, thus enhancing the gas-liquid mass transfer. The hydrodynamic effect relates to the

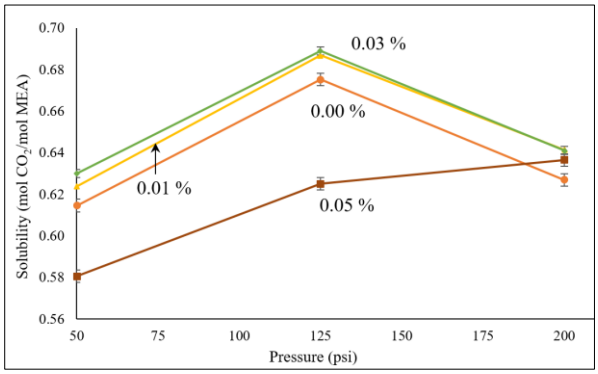

Figure 6. CO_2 solubility of nanofluids.

diffusion boundary layer of a gas-liquid system. The presence of nanoparticles induces Brownian motion, microconvections, and velocity disturbances, which affect the diffusion boundary layer and reduce its thickness. The bubbles of the gas molecules collide with nanoparticles and break into smaller bubbles. Smaller bubbles increase the gas-liquid contact area, thereby enhancing the mass transfer. This phenomenon is called the inhibition of bubble coalescence. Adding GNPs enhances the mass transfer of MEA through the mass transfer enhancement mechanisms. The effect becomes greater as the concentration of solid increases. However, when the solid loading is too high, the gas-liquid interfacial area is limited, and adjacent particles may be exposed to form a "plate", which can hinder mass transfer (Jiang et al., 2014). Combining these two effects leads to an increment, followed by a reduction in the enhancement factor with the concentration of the GNP nanoparticles. The highest enhancement result of CO_2 solubility at each concentration of GNPs can be observed at 125 psi (862 kPa).

5. Conclusion

In this study, GNP-MEA nanofluids were prepared, and its performance in CO_2 absorption was studied. The characterization revealed typical characteristics of GNPs. The experimental data revealed that the addition of GNPs increased the performance of MEA for CO_2 absorption by 2%. For the effect of nanoparticle concentrations, the CO_2 absorptivity of MEA increased with increasing concentrations until the optimum concentration was reached. The enhancement of MEA performance in CO_2 absorption was related to the generally acknowledged mass transfer enhancement mechanisms. Therefore, the suspensions of GNPs in MEA are expected to enhance CO_2 absorption.

6. Acknowledgements

Dr. A. Arifutzzaman and Professor Mohamed Kheireddine Aroua would like to acknowledge the financial support provided by Sunway University, Malaysia, through the internal grant project No. # GRTIN-IGS-CCDCU[S]-09-2022.

7. References

Abdul Samat, N. F. N., Yusoff, R. B., Aroua, M. K., Ramalingam, A., & Kassim, M. A. (2019). Solubility of CO2 in aqueous 2-amino-1, 3-propanediol (Serinol) at elevated pressures. *Journal of Molecular Liquids, 277*, 207-216. doi: https://doi.org/10.1016/j.molliq.2018.12.102

Farinre, O. Z., Alghamdi, H., Kelley, M. L., Biacchi, A. J., Albert, V., Davydov, . . . Misra, P. (2022). *A Comprehensive Study on the Molecular Dynamics of Pristine and Functionalized Graphene Nanoplatelets*.

Gomari, S., Esfandeh, M., & Ghasemi, I. (2017). All-solid-state flexible nanocomposite polymer electrolytes based on poly(ethylene oxide): Lithium perchlorate using functionalized graphene. *Solid State Ionics, 303*, 37-46. doi: https://doi.org/10.1016/j.ssi.2017.02.005

Hamidi, R., Farsi, M., & Eslamloueyan, R. (2018). CO2 solubility in aqueous mixture of MEA, MDEA and DAMP: Absorption capacity, rate and regeneration. *Journal of Molecular Liquids, 265*, 711-716. doi: https://doi.org/10.1016/j.molliq.2018.07.013

Jiang, J., Zhao, B., Zhuo, Y., & Wang, S. (2014). Experimental study of CO2 absorption in aqueous MEA and MDEA solutions enhanced by nanoparticles. *International Journal of greenhouse gas control, 29*, 135-141.

Kumar, J. S., Murmu, N. C., Samanta, P., Banerjee, A., Ganesh, R. S., Inokawa, H., & Kuila, T. (2018). Novel synthesis of a Cu2O–graphene nanoplatelet composite through a two-step electrodeposition method for selective detection of hydrogen peroxide. *New Journal of Chemistry, 42*(5), 3574-3581. doi: 10.1039/C7NJ04510G

Lai, Q., Toan, S., Assiri, M. A., Cheng, H., Russell, A. G., Adidharma, H., . . . Fan, M. (2018). Catalyst-TiO(OH)2 could drastically reduce the energy consumption of CO2 capture. *Nature Communications, 9*(1), 2672. doi: 10.1038/s41467-018-05145-0

Mohammadpoor, A., Mirzaei, M., Azimi, A., & ghomshe, m. t. (2018). The simultaneous effect of graphene oxide and sodium dodecyl sulphate nanoparticles on the kinetics of CO2 absorption in amine. *Advances in environmental science and technology, 4*, 163-174.

Mohammadpour, A., Mirzaei, M., & Azimi, A. (2019). Dimensionless numbers for solubility and mass transfer rate of CO2 absorption in MEA in presence of additives. *Chemical Engineering Research and Design, 151*, 207-213. doi: https://doi.org/10.1016/j.cherd.2019.06.026

DOI: https://doi.org/10.22452/mjs.vol43sp1.3
Malaysian Journal of Science 43 (Special Issue 1): 15-19 (July 2024)

Ochedi, F. O., Yu, J., Yu, H., Liu, Y., & Hussain, A. (2021). Carbon dioxide capture using liquid absorption methods: a review. *Environmental Chemistry Letters, 19*, 77-109.

Rahimi, K., Riahi, S., & Abbasi, M. (2020). Effect of host fluid and hydrophilicity of multi-walled carbon nanotubes on stability and CO2 absorption of amine-based and water-based nanofluids. *Journal of Environmental Chemical Engineering, 8*(1), 103580. doi: https://doi.org/10.1016/j.jece.2019.103580

Ramezani, R., Mazinani, S., & Di Felice, R. (2021). Density, Viscosity, pH, Heat of Absorption, and CO2 Loading Capacity of Methyldiethanolamine and Potassium Lysinate Blend Solutions. *Journal of Chemical & Engineering Data, 66*(4), 1611-1629.

Seo, S., Lages, B., & Kim, M. (2020). Catalytic CO2 absorption in an amine solvent using nickel nanoparticles for post-combustion carbon capture. *Journal of CO2 Utilization, 36*, 244-252.

Zhang, H., Wang, B., Xiong, M., Gao, C., Ren, H., & Ma, L. (2022). Process intensification in gas-liquid mass transfer by nanofluids: Mechanism and current status. *Journal of Molecular Liquids, 346*, 118268.

DOI: https://doi.org/10.22452/mjs.vol43sp1.3
Malaysian Journal of Science 43 (Special Issue 1): 15-19 (July 2024)